CHEMISTRY
A European Journal

A Journal of
ChemPubSoc Europe

Accepted Article

Title: Anisotropic Thermal and Guest-Induced Responses of an Ultramicroporous Framework with Rigid Linkers

Authors: Josie E. Auckett, Samuel G. Duyker, Ekaterina I. Izgorodina, Chris S. Hawes, David R. Turner, Stuart R. Batten, and Vanessa Kate Peterson

To be cited as: *Chem. Eur. J.* 10.1002/chem.201800261

Link to VoR: http://dx.doi.org/10.1002/chem.201800261

Supported by
ACES

WILEY-VCH

10.1002/chem.201800261

WILEY-VCH

Anisotropic Thermal and Guest-Induced Responses of an Ultramicroporous Framework with Rigid Linkers

Josie E. Auckett, Samuel G. Duyker, Ekaterina I. Izgorodina, Chris S. Hawes[†], David R. Turner, Stuart R. Batten, and Vanessa K. Peterson*

Abstract: The interdependent effects of temperature and guest uptake on the structure of the ultramicroporous metal-organic framework $[Cu_3(cdm)_4]$ (cdm = $C(CN)_2(CONH_2)^-$) are explored in detail using *in situ* neutron scattering and density functional theory calculations. The tetragonal lattice displays an anisotropic thermal response related to a hinged "lattice-fence" mechanism, unusual for this topology, which is facilitated by pivoting of the rigid cdm anion about the Cu nodes. Calculated pore size metrics clearly illustrate the potential for temperature-mediated adsorption in ultramicroporous frameworks due to thermal fluctuations of the pore diameter near the value of the target guest kinetic diameter, though in $[Cu_3(cdm)_4]$ this is counteracted by a competing contraction of the pore with increasing temperature as a result of the anisotropic lattice response.

Microporous framework solids have shown promising performance in the realm of gas sorption, where selective and efficient uptake is highly desirable for achieving a wide range of industrial gas separations.[1] Metal-organic frameworks (MOFs) have attracted particular attention in this area due to the exceptional tunability of their pore shape, size, and chemistry, which can be used to improve separation performance by targeting differences in the physical (size, shape) or chemical (polarity, polarizability) characteristics of competing guests.[1b] Host-guest interactions in porous systems must be well understood in order for such tuning to be accomplished effectively, as the steric and chemical interactions of the guest molecules can significantly perturb the host framework structure and dynamics. Indeed, while the responsiveness of framework materials to external stimuli such as temperature,[2] pressure,[3] light,[4] or magnetic field[5] may be exploited to trigger the uptake or removal of guests on demand, the possibility for guest uptake itself to act as a stimulus for the modification of framework structures and properties is beginning to be explored.[6]

The inherent physical flexibility of many MOFs compared to traditional sorbents (e.g. zeolites)[7] provides another important pathway for optimizing function, not only because framework flexibility has been shown to facilitate guest selectivity in several important MOF systems,[8] but also because of its bearing on fundamental behaviors such as thermal expansion.[9] Negative thermal expansion (NTE) occurs in many porous frameworks as a result of various mechanisms of interaction between rigid and flexible structural components and the empty pore spaces.[10] Tunable thermal expansion is of particular interest in the development of zero thermal expansion (ZTE) materials for various functional devices that must be robust to operational temperature cycling.

A new ultramicroporous MOF, $[Cu_3(cdm)_4]$ (hereafter **1**; cdm = carbamoyldicyanomethanide, $C(CN)_2(CONH_2)^-$), was recently reported.[11] Porosity in desolvated **1** manifests as one-dimensional, non-intersecting zig-zag channels of 3–4 Å diameter which are interleaved along the *a* and *b* directions of the tetragonal unit cell (Figure 1). Square-planar-coordinated Cu^{II} atoms are positioned at the corners of these zig-zag channels with these exposed to the pore space, creating a high concentration of vacant sites for axial guest binding along the channel walls. The lattice of **1** exhibits positive thermal expansion (PTE) along the *c* axis and NTE in the *a*-*b* plane.[12] Although the presence of adsorbed CO_2 has been shown to influence the rate of thermal expansion,[12] no detailed investigation into the interactions between the guest molecules and the structural features responsible for anisotropic thermal expansion (ATE) in **1** has yet been reported.

The similarity between the diameters of small gas molecules (CO_2, N_2, CH_4, etc.) and the channel diameter of **1** suggests the possibility of temperature- or even guest-influenced "sieving" behavior, as modest structural changes might be sufficient to trigger size-based acceptance or rejection of a target guest species. The work of Chevreau *et al*. demonstrates that the unusual thermal response of the lattice is also somewhat sensitive to guest loading.[12] We were therefore motivated to investigate the temperature evolution of the crystal lattice and

[*] Dr J. E. Auckett, Prof. V. K. Peterson
Australian Centre for Neutron Scattering, Australian Nuclear Science and Technology Organisation, New Illawarra Rd, Lucas Heights, New South Wales 2234, Australia
E-mail: Vanessa.peterson@ansto.gov.au
Dr S. G. Duyker
School of Chemistry
The University of Sydney
New South Wales 2006, Australia
Assoc. Prof. E. I. Izgorodina, Dr C. S. Hawes, Dr D. R. Turner, Prof. S. R. Batten
School of Chemistry
Monash University
Victoria 3800, Australia
[†] Present address: School of Chemical and Physical Sciences
Keele University
Staffordshire ST5 5BG, United Kingdom

Supporting information for this article is given via a link at the end of the document.

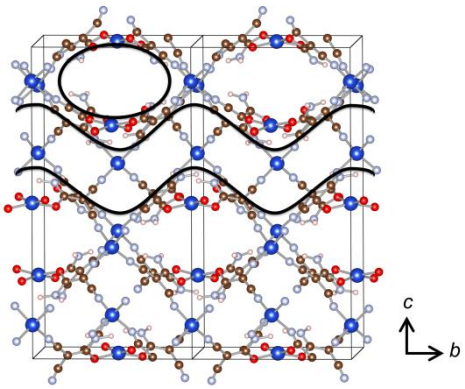

Figure 1. (The crystal structure of **1** (two unit cells are shown). Curved lines indicate the approximate form of the interleaved 1D zig-zag channels extending in the *a* and *b* directions. Structure was visualized using VESTA.[15]

pore dimensions of **1** in more detail.

The lattice parameters of **1** obtained from Rietveld refinements against variable-temperature neutron powder diffraction (NPD) data are presented in Figure 2. A typical Rietveld plot shown in Figure 3. All observed trends agree closely with those reported previously for Le Bail analysis of the same data.[12] Below ~50 K, an unusual reversal of lattice expansion is observed such that the values of the *a* and *c* parameters at 15 K are most similar to those measured at 80 K. The volumetric coefficient of thermal expansion (α_V = (1/*V*)(d*V*/d*T*)) is positive at all temperatures, but the contributions of a^2 and *c* are virtually equal and opposite below 120 K, giving rise to near-zero volumetric thermal expansion (ZTE) in this temperature range (Table 1). Above ~120 K, a^2 and *c* both vary more rapidly with temperature, with the greater increase in magnitude of α_c resulting in significantly positive volume expansion. The values α_a = –18.8(6) MK^{-1} and α_c = 46.8(19) MK^{-1} obtained in this range are characteristic of moderately flexible MOFs.[13] It should also be noted that areal NTE (that is, NTE along two orthogonal crystal axes) is relatively uncommon among ATE materials, the magnitude of the negative coefficient α_{a2} = –37.5(13) MK^{-1} having been exceeded on only a few occasions.[13-14] The introduction of CO_2 into the pores of **1** accelerates both the negative expansion of *a* and the positive expansion of *c* (see Table S1 in the Supporting Information), but the general character of lattice expansion is unaltered, and slight gradient changes near 50 K and 120 K are still observed.

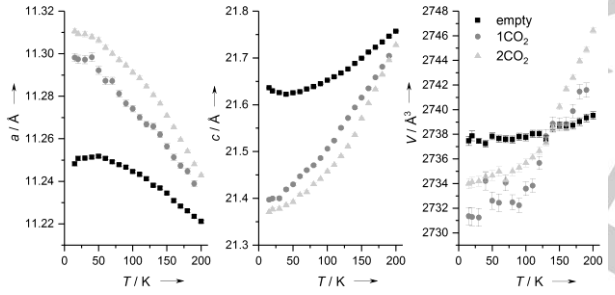

Figure 2. The lattice parameters of $[Cu_3(cdm)_4]$ (empty) and with 1 and 2 CO_2 molecules adsorbed per $[Cu_3(cdm)_4]$ unit ($1CO_2$ and $2CO_2$, respectively) refined against NPD data.

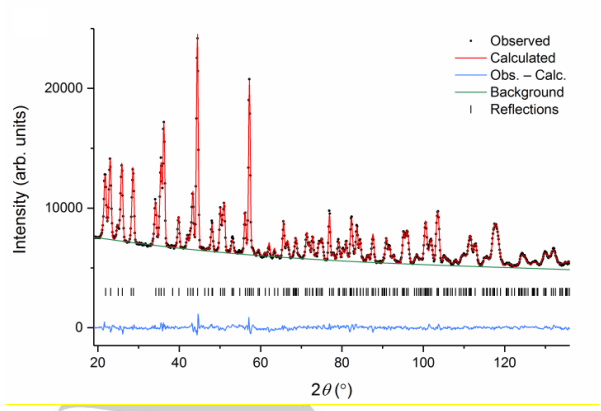

Figure 3. Rietveld refinement profile for the empty framework of **1** against NPD data collected at 15 K. (wR = 1.66% for 56 refined parameters)

Identifying the mechanism of areal NTE in **1** is made difficult by its topological complexity; each planar cdm ligand bridges one Cu^{II} (square-planar) and two Cu^{I} (tetrahedral) nodes and is not aligned with any crystallographic axis, so that the direct effect of a changing bond length or angle on the lattice parameters *a* and *c* cannot be easily predicted. Inspection of structural parameters refined against the NPD data reveals that the isotropic atomic displacement parameters (ADPs) of the C1, C3, and N3 sites increase more rapidly with temperature than those of other linker atoms, suggesting a greater degree of thermal motion or disorder (Figure 4). *Ab initio* geometry optimizations of cdm-Cu units and clusters performed using Gaussian09[16] show that the cdm anion remains rigid and planar even when coordinated in a network of Cu^{I} and Cu^{II} nodes; natural bond order analysis reveals that this is due to delocalization of electrons over the whole anion, reinforced by significant charge transfer of up to 0.18 *e* between the Cu^{I} atoms and coordinating N atoms (see Supporting Information). The calculations imply that the increased observed displacement of C1, C3, and N3 arises from a rigid tilt or rotation of the cdm ligand relative to the Cu nodes. The data in Figure 4(c) suggest that the O site (adjacent to -C3-N3) is moderately displaced, while the -C2-N2 "arm" is the most stationary. The more constricted local environment of -C2-N2 (Supplementary Figure S3) presumably forces the anion to pivot from this side, while the -C3-N3 side having access to the pore space can swing more freely.

The dynamic deformation of **1** was examined by calculating the mean and standard deviation of bond lengths and angles aggregated over density functional theory based molecular

Table 1. Coefficients of thermal expansion of **1** obtained from linear fits to the refined lattice parameters. The linear fits yielding these coefficients are depicted in the Supporting Information (Figure S2).

	15 ≤ T ≤ 50 K	50 ≤ T ≤ 120 K	120 ≤ T ≤ 350 K
α_{a2} (MK^{-1})	12(6)	–26.7(9)	–37.5(13)
α_c (MK^{-1})	–13(6)	28.5(15)	46.8(18)
α_V (MK^{-1})	1(4)	1.7(9)	9.3(9)

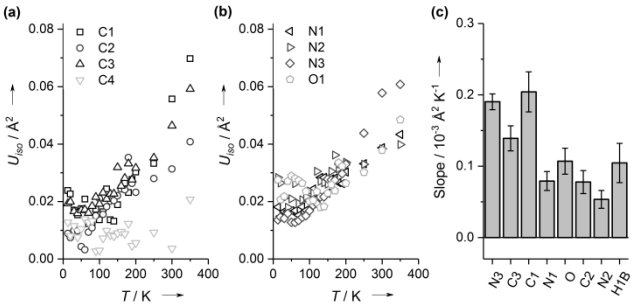

Figure 4. (a, b) Refined isotropic ADPs for selected atoms in **1**. Error bars (on the order of ~ 0.01 $Å^2$) are omitted for clarity. (c) Gradients of linear regression fits to the U_{iso} values in the range 120–350 K. Atoms for which the linear fit quality R^2 < 50% are not shown.

dynamics (MD) simulations performed using VASP.[17] Consideration of a simplified topological framework consisting of only C1, C4, and the Cu nodes (Figure 5) reveals a clear decrease of Cu1–C1 distances upon heating to 273 K, despite the fact that all individual bonds along these linkages either lengthen (N--Cu1) or remain unchanged (C≡N and C–C1) (Figure 6). The combination of topological changes summarized in Figure 5 is consistent with either a displacement of the cdm ligand towards the Cu1--Cu1 axis and away from Cu2, or a clockwise in-plane rotation of cdm around a point near the -C2-N2 arm.

Several angles whose bisectors lie closer to the *c* axis (e.g. C4–Cu2–C4 (trans), C1–(3)–Cu1–(3)–C1 and C1–(2)–Cu1–(2)–C1) are observed to decrease slightly at 273 K, while the Cu1–C1–Cu1 angle (bisected in the *a*-*b* plane) increases slightly. These changes to the environments of the Cu nodes, especially Cu1, hint at a topologically complicated version of the "wine rack" or "lattice fence" behavior found in the great majority of molecular frameworks which exhibit simultaneous PTE/NTE. In the typical mechanism, the vertices of diamond-shaped motifs act as flexible hinges to produce cooperative expansion and contraction in orthogonal directions.[6a, 9, 18] Previously known examples of this tend to have much simpler topologies, often constructed of parallel four-sided channels with metal ions or clusters located at the corners.[18-19] Many also contain large, flexible ligands which may themselves act as hinges,[9] or trivial ligands with few degrees of freedom.[10a, 20] The particular rigidity of the 10-atom planar cdm anion allows it to act as a rigid, pseudo-triangular strut and facilitate areal NTE within the three-dimensional topology of **1** in a new application of this mechanism. Indeed, the lack of flexibility of cdm combined with the strongly interconnected topology may be speculated to drive ATE in **1,** as the framework attempts to accommodate increasing dynamic motion of the rigid cdm units without breaking topology or deforming the linkers.

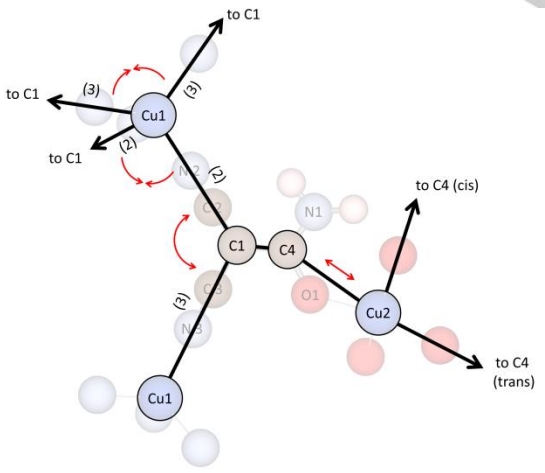

Figure 5. Simplified topology of **1** used for the calculation of interatomic distances and angles in the lower panels of Figure 6. Small red arrows indicate the direction of change of select distances and angles with increasing temperature.

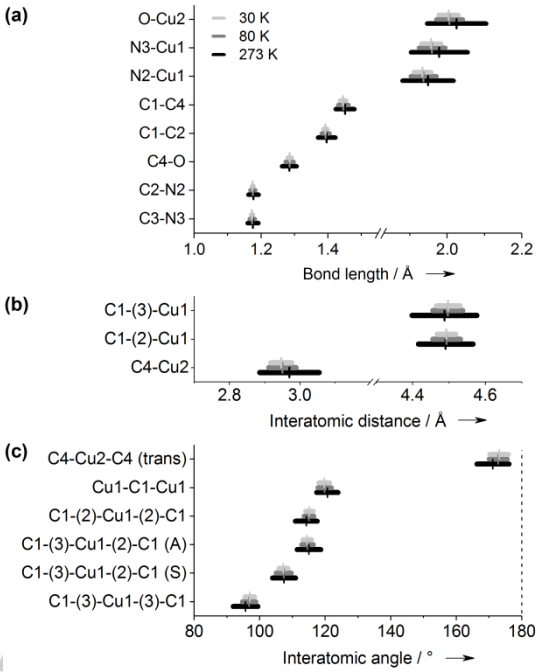

Figure 6. Mean (vertical symbols) and standard deviation (horizontal bars = 2σ) of selected interatomic distances and angles during MD simulations of the empty framework at 30, 80, and 273 K. The numbers (2) and (3) indicate whether the interatomic distance corresponds to a C1-(C2N2)-Cu1 or a C1-(C3N3)-Cu1 linkage, respectively (see Figure 5). For angles involving the -(2)-Cu1-(3)- linkage, the letters (S) and (A) denote whether the two arms of the angle lie alongside the same channel or adjacent channels, respectively.

In order to assess the effects of the temperature- and guest-induced structural changes on guest uptake and diffusion in **1**, detailed pore size analysis was carried out using the Zeo++ software package.[21] Dynamic distributions of the maximum pore size (MPS) and limiting pore size (LPS) were extracted from the MD simulation trajectories at 30, 80, and 273 K and fitted using either symmetric or asymmetric peak functions as appropriate (Figure 7). Descriptions and locations of these pore size metrics can be found in the supporting information. The widths of these dynamic distributions increased considerably with temperature for both the empty and CO_2-dosed structures, reflecting increased thermal motion of the framework. Broadening was also evident upon isothermal CO_2 uptake, probably as a result of increased structural disorder due to the partial occupancy of the eight available Site 1-type CO_2 binding locations in the simulated unit cell. The center of the dynamic MPS distribution was found to be largely temperature-independent for the empty framework, and also insensitive to the presence of CO_2 at ≤ 80 K. By contrast, the LPS distribution showed a clear negative shift with increasing temperature (Figure 7) which was most pronounced for the empty framework (~ −0.1 Å from 30 to 80 K).

The temperature-induced broadening of the LPS distribution provides a graphical illustration of the potential for temperature-driven size selection in ultramicroporous materials such as **1**, in cases where the kinetic diameter of a target molecule exceeds the LPS distribution at low temperatures but is overlapped by the distribution at higher temperatures. However, despite the

promise offered by the similarity of the kinetic diameter of CO_2 (3.3 Å) to the LPS of **1**, the stability of the upper dynamic LPS values appears to negate the possibility of thermally "switching" the diffusion ability of CO_2 (or any other guest molecules) in the pores of **1** within the investigated temperature range.

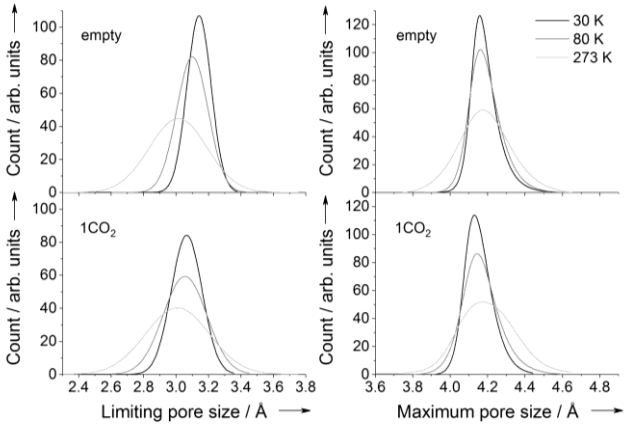

Figure 7. Distribution curves fitted to the histograms of pore size values sampled from the MD simulations of **1**. The fitted functions are Gaussian (for LPS) or asymmetric double Sigmoidal (for MPS; see Supporting Information). The raw histograms are presented in Supplementary Figure S8.

In conclusion, experimental and theoretical investigations show that the response of the ultramicroporous $[Cu_3(cdm)_4]$ framework to temperature and to adsorbed CO_2 is complex and offers several features of interest. Detailed examination of the temperature-dependent positions and dynamic motions of the framework atoms shows that significant areal negative thermal expansion arises from a complicated "lattice fence"-type hinging around the Cu nodes, with the cdm anions acting as rigid struts which pivot asymmetrically about these nodes. Importantly, the changing aspect ratio of the unit cell does not substantially alter the diameter of the minimum aperture allowing guests to diffuse through the pores, as the increased thermal fluctuations of this aperture are counteracted by an overall contraction of the pore with increasing temperature. Nevertheless, the potential for thermal fluctuations of the diffusion-limiting pore aperture to enable temperature-triggered adsorption in other ultramicroporous materials, especially where the LPS is very close to the guest kinetic diameter, is clearly illustrated.

Acknowledgements

This research was supported by the Science and Industry Endowment Fund (RP02-035). We thank the sample environment team at the Australian Centre for Neutron Scattering for assistance and support with respect to the gas-delivery equipment used for the NPD experiment.

Keywords: density functional calculations • gas sorption • metal-organic frameworks • negative thermal expansion • neutron diffraction

[1] a) J.-R. Li, R. J. Kuppler, H.-C. Zhou, *Chem. Soc. Rev.* **2009**, *38*, 1477-1504; b) C. H. Hendon, A. J. Rieth, M. D. Korzyński, M. Dincă, *ACS Cent. Sci.* **2017**, *3*, 554-563.
[2] J. A. Mason, K. Sumida, Z. R. Herm, R. Krishna, J. R. Long, *Energy Environ. Sci.* **2011**, *4*, 3030-3040.
[3] S. G. Duyker, V. K. Peterson, G. J. Kearley, A. J. Studer, C. J. Kepert, *Nat. Chem.* **2016**, *8*, 270-275.
[4] a) J. Park, D. Yuan, K. T. Pham, J. R. Li, A. Yakovenko, H. C. Zhou, *J. Am. Chem. Soc.* **2012**, *134*, 99-102; b) R. Lyndon, K. Konstas, B. P. Ladewig, P. D. Southon, C. J. Kepert, M. R. Hill, *Angew. Chem. Int. Ed.* **2013**, *52*, 3695-3698.
[5] a) H. Li, M. M. Sadiq, K. Suzuki, R. Ricco, C. Doblin, A. J. Hill, S. Lim, P. Falcaro, M. R. Hill, *Adv. Mater.* **2016**, *28*, 1839-1844; b) M. M. Sadiq, H. Li, A. J. Hill, P. Falcaro, M. R. Hill, K. Suzuki, *Chem. Mater.* **2016**, *28*, 6219-6226.
[6] a) H.-L. Zhou, R.-B. Lin, C.-T. He, Y.-B. Zhang, N. Feng, Q. Wang, F. Deng, J.-P. Zhang, X.-M. Chen, *Nat. Commun.* **2013**, *4*, 2534; b) N. Yanai, T. Uemura, M. Inoue, R. Matsuda, T. Fukushima, M. Tsujimoto, S. Isoda, S. Kitagawa, *J. Am. Chem. Soc.* **2012**, *134*, 4501-4504; c) P. Canepa, K. Tan, Y. Du, H. Lu, Y. J. Chabal, T. Thonhauser, *J. Mater. Chem. A* **2015**, *3*, 986-995.
[7] A. J. Fletcher, K. M. Thomas, M. J. Rosseinsky, *J. Solid State Chem.* **2005**, *178*, 2491-2510.
[8] a) L. Hamon, P. L. Llewellyn, T. Devic, A. Ghoufi, G. Clet, V. Guillerm, G. D. Pirngruber, G. Maurin, C. Serre, G. Driver, W. Van Beek, E. Jolimaître, A. Vimont, M. Daturi, G. Férey, *J. Am. Chem. Soc.* **2009**, *131*, 17490-17499; b) D. Peralta, G. Chaplais, A. Simon-Masseron, K. Barthelet, C. Chizallet, A.-A. Quoineaud, G. D. Pirngruber, *J. Am. Chem. Soc.* **2012**, *134*, 8115-8126.
[9] L. D. DeVries, P. M. Barron, E. P. Hurley, C. Hu, W. Choe, *J. Am. Chem. Soc.* **2011**, *133*, 14848-14851.
[10] a) A. L. Goodwin, K. W. Chapman, C. J. Kepert, *J. Am. Chem. Soc.* **2005**, *127*, 17980-17981; b) J. Chen, L. Hu, J. Deng, X. Xing, *Chem. Soc. Rev.* **2015**, *44*, 3522-3567.
[11] L. J. McCormick, S. G. Duyker, A. W. Thornton, C. S. Hawes, M. R. Hill, V. K. Peterson, S. R. Batten, D. R. Turner, *Chem. Mater.* **2014**, *26*, 4640-4646.
[12] H. Chevreau, S. G. Duyker, V. K. Peterson, *Acta Crystallogr. Sect. B* **2015**, *71*, 648-660.
[13] S. A. Hodgson, J. Adamson, S. J. Hunt, M. J. Cliffe, A. B. Cairns, A. L. Thompson, M. G. Tucker, N. P. Funnell, A. L. Goodwin, *Chem. Commun.* **2014**, *50*, 5264-5266.
[14] a) M. J. Cliffe, A. L. Goodwin, *J. Appl. Crystallogr.* **2012**, *45*, 1321-1329; b) S. J. Hunt, M. J. Cliffe, J. A. Hill, A. B. Cairns, N. P. Funnell, A. L. Goodwin, *CrystEngComm* **2015**, *17*, 361-369; c) J. Pang, C. Liu, Y. Huang, M. Wu, F. Jiang, D. Yuan, F. Hu, K. Su, G. Liu, M. Hong, *Angew. Chem. Int. Ed.* **2016**, *55*, 7478-7482.
[15] K. Momma, F. Izuma, *J. Appl. Crystallogr.* **2008**, *41*, 653-658.
[16] G. W. T. M. J. Frisch, H. B. Schlegel, G. E. Scuseria, M. A. Robb, J. R. Cheeseman, G. Scalmani, V. Barone, G. A. Petersson, H. Nakatsuji, X. Li, M. Caricato, A. Marenich, J. Bloino, B. G. Janesko, R. Gomperts, B. Mennucci, H. P. Hratchian, J. V. Ortiz, A. F. Izmaylov, J. L. Sonnenberg, D. Williams-Young, F. Ding, F. Lipparini, F. Egidi, J. Goings, B. Peng, A. Petrone, T. Henderson, D. Ranasinghe, V. G. Zakrzewski, J. Gao, N. Rega, G. Zheng, W. Liang, M. Hada, M. Ehara, K. Toyota, R. Fukuda, J. Hasegawa, M. Ishida, T. Nakajima, Y. Honda, O. Kitao, H. Nakai, T. Vreven, K. Throssell, J. A. Montgomery, Jr., J. E. Peralta, F. Ogliaro, M. Bearpark, J. J. Heyd, E. Brothers, K. N. Kudin, V. N. Staroverov, T. Keith, R. Kobayashi, J. Normand, K. Raghavachari, A. Rendell, J. C. Burant, S. S. Iyengar, J. Tomasi, M. Cossi, J. M. Millam, M. Klene, C. Adamo, R. Cammi, J. W. Ochterski, R. L. Martin, K. Morokuma, O. Farkas, J. B. Foresman, and D. J. Fox, Gaussian, Inc., Wallingford CT, 2016.
[17] a) G. Kresse, J. Furthmuller, *Comput. Mater. Chem.* **1996**, *6*, 15-50; b) G. Kresse, J. Furthmuller, *Phys. Rev. B* **1996**, *54*, 11169-11186; c) G. Kresse, J. Hafner, *Phys. Rev. B* **1993**, *47*, 558-561.
[18] J. M. Ogborn, I. E. Collings, S. A. Moggach, A. L. Thompson, A. L. Goodwin, *Chem. Sci.* **2012**, *3*, 3011-3017.
[19] A. Kondo, K. Maeda, *J. Solid State Chem.* **2015**, *221*, 126-131.
[20] A. B. Cairns, A. L. Thompson, M. G. Tucker, J. Haines, A. L. Goodwin, *J. Am. Chem. Soc.* **2012**, *134*, 4454-4456.
[21] T. F. Willems, C. H. Rycroft, M. Kazi, J. C. Meza, M. Haranczyk, *Microporous Mesoporous Mater.* **2012**, *149*, 134-141.

10.1002/chem.201800261

WILEY-VCH

Entry for the Table of Contents

COMMUNICATION

The metal-organic framework $[Cu_3(cdm)_4]$ exhibits areal negative thermal expansion over a broad temperature range. *In situ* neutron scattering and density functional theory calculations provide considerable insight into the underlying atomistic causes of this phenomenon, the influence of adsorbed guest molecules, and the implications for potential temperature-mediated adsorption in ultramicroporous frameworks.

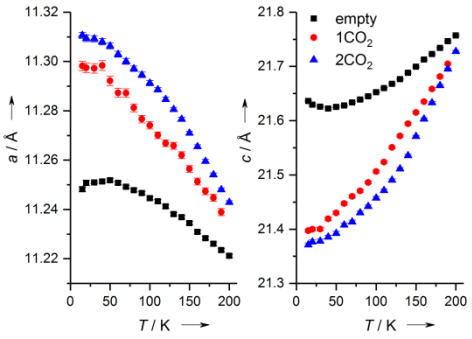

*Josie E. Auckett, Samuel G. Duyker, Ekaterina I. Izgorodina, Chris S. Hawes, David R. Turner, Stuart R. Batten, and Vanessa K. Peterson**

Page No. – Page No.

Anisotropic Thermal and Guest-Induced Responses of an Ultramicroporous Framework with Rigid Linkers